Utilization of waste tea leaves as bio-surfactant in CdS quantum dots synthesis and their cytotoxicity effect in breast cancer cells

Kavitha Shivaji, Mythili Gnanamangai Balasubramanian, Anitha Devadoss, Vijayshankar Asokan, Catherine Suenne De Castro, Matthew Lloyd Davies, Ponnusammy Ponmurugan, Sudhagar Pitchaimuthu

PII: S0169-4332(19)31357-1
DOI: https://doi.org/10.1016/j.apsusc.2019.05.050
Reference: APSUSC 42636

To appear in: *Applied Surface Science*

Received date: 12 February 2019
Revised date: 9 April 2019
Accepted date: 6 May 2019

Please cite this article as: K. Shivaji, M.G. Balasubramanian, A. Devadoss, et al., Utilization of waste tea leaves as bio-surfactant in CdS quantum dots synthesis and their cytotoxicity effect in breast cancer cells, Applied Surface Science, https://doi.org/10.1016/j.apsusc.2019.05.050

Utilization of Waste Tea Leaves as Bio-surfactant in CdS Quantum Dots Synthesis and their Cytotoxicity Effect in Breast Cancer Cells

Kavitha Shivaji,[a] Mythili Gnanamangai Balasubramanian,[a] Anitha Devadoss,[b] Vijayshankar Asokan,[c] Catherine Suenne De Castro,[d] Matthew Lloyd Davies,[d] Ponnusammy Ponmurugan,[e] and Sudhagar Pitchaimuthu[d]*

[a] *Department of Biotechnology, K.S.Rangasamy College of Technology, Tiruchengode. 637215, Tamil Nadu. India.*

[b] *Centre for Nano Health, College of Engineering, Swansea University, Singleton Park, Swansea, SA2 8PP, Wales, United Kingdom.*

[c] *Environmental Inorganic Chemistry, Department of Chemistry and Chemical Engineering, Chalmers University of Science and Technology, Gothenburg, Sweden. SE-41296*

[d] *SPECIFIC, Materials Research Centre, College of Engineering, Swansea University (Bay Campus), Fabian Way, Swansea SA1 8EN, United Kingdom.*

[e] *Department of Botany, Bharathiar University, Coimbatore, India*

*Corresponding Author: S.Pitchaimuthu@swansea.ac.uk

Abstract

Green technology for nanoparticles synthesis is considered to be of great significance in biomedical applications. Recently, low dimensional semiconductor cadmium sulfide (CdS) quantum dots (QDs) have raised great attention due to their optical properties and wide usage in biomedical studies. In our present work, we demonstrate a simple green synthesis route for CdS QDs production using waste matured tea leaves (mother leaf) as bio-surfactant that are a waste product of the tea leaf industry and not suitable for drinking. The structural and morphological analysis showed waste tea leaf derived CdS QDs range from 2.5 to 4 nm in particle size with a cubic crystalline structure. Interestingly, these CdS QDs exhibit strong florescence emission with maximum around 670 nm. We explored the cytotoxic effect of waste tea leaf mediated CdS QDs (MT-CdS QDs) in breast cancer cell lines and compared their viability with standard drug - cisplatin. Our experimental studies strongly suggest that MT-CdS QDs exhibits cytotoxic effect on breast cancer cells and their performance was compared with standard drug cisplatin. To further understand the role of MT-CdS QDs towards cytotoxicity, the fluorescence microscopy and flow cytometry analysis were carried out. The flow cytometry results reveal that MT-CdS QDs induces cell death as it arrests the cell cycle at S phase as well as G2/M phase. Further the apoptosis mechanism was confirmed with the expression of anti-apoptotic and apoptotic proteins. These studies explored that waste tea leaves have dual advantage – both in controlling the particle size of CdS QDs as well as facilitates their cytotoxicity effect in breast cancer cell death. Therefore, it is anticipated that the utilization of MT-CdS QDs produced from waste tea leaves as bi-functional drug and delivery vehicle in cancer treatment will be a promising approach. Also, this is a simple and circular economic route for producing biocompatible QDs at low-cost, which could simultaneously benefit tea and biomedical industries.

KEYWORDS: Quantum dots, CdS, Waste tea leaves, green synthesis, breast cancer, apoptosis, cytotoxicity.

1. Introduction

Cancer is a foremost public health issue with a high mortality around the globe. Particularly, breast cancer is the second most common cancer-causing death in women both in developed and under-developed countries. Breast cancer is a tumor developed from the breast tissue. Currently chemo and radio therapeutic options are available for cancer treatment, however, these treatments adversely affect the healthy cells too. Recent developments in bio-nanomedicine makes it a promising route to tackle the cancer through selective therapy using low-dimension nanoparticle as drug delivery vehicles. For instance, target drug embedded nanoparticle vehicles selectively identify the tumor cells and deliver the drugs without affecting the healthy cells [1-4]. In the past two decades, a wide range of research was devoted towards exploring the application of semiconductor quantum dots (QDs) as multifunctional theragnostic tool in cancer diagnosis and treatment [5-7]. The smaller QDs size (1-10 nm) attracts as bio-vehicle to identify the cancer cells compared to organic fluorophores [8]. In associate with targeting ligands or molecule functionalization, the QDs can penetrate the cancer cell and effectively deliver the drug [9]. For instance, graphene quantum dots conjugated with standard drug cisplatin promotes cellular uptake that results in high cytotoxic effect on lung cancer cells, [10] which attests that the QDs are promising drug delivery vehicles in cancer treatment. In addition, QDs can produce reactive oxygen species (ROS), which can destroy the cancer cells [1, 11].

Light active QD based photodynamic therapy is yet another promising example of applying the QDs as drugs in cancer cells treatment [12, 13]. However, the stability of QDs in chemical reaction is a challenging issue, which would affect their performance in cancer cell diagnosis and treatment. Significant post-treatment approaches have been developed for the surface protection and stabilization of QDs using polymers, micelles and ligands [14-16]. Therefore, the cellular uptake of QDs rely on size [17], shape [18, 19], and surface functionalization [20]. Though the surface modification enhances the QDs stability, the biocompatibility nature of chemically synthesized QDs limits their application as it involves toxic organic chemicals [21-23]. In this line, plant extract derived QDs synthesis is an attractive, toxic-free, green approach compared to conventional chemical synthesis, [24-27] where, the organic moieties present in the plant extract acts as bio-surfactant and stabilize the QDs. Among the semiconductor QDs, cadmium sulphide (CdS) QDs showed wide range of applications such as display devices, solar cells, solar fuel generation, cancer cell and stem cell imaging, and photodynamic therapy [28-32]. Singh *et. al.* reported bio-surfactant assisted CdS QDs induced cell death in prostate cancer cells via p53, Bcl-2 and caspase pathway by ROS mediated oxidative stress [33].

In our previous study, we have demonstrated the utilization of young tea leaves (*camellia sinesis*) extract as bio-surfactant for producing biocompatible CdS QDs in the range between 3-5 nm [34]. These tea leaves mediated CdS QDs exhibited multifunctional properties such as antibacterial and anticancer effect against lung cancer cells with better fluorescence properties. It is found that the rich phytochemicals (polyphenols, vitamins, carbohydrates, minerals and caffeine) present in the young tea leaves were responsible for downsizing the QDs. Although these young tea leaves derived QDs show superior performance, from circular economy view

point this wouldn't be ideal. As, the young tea leaves have been consumed as beverage all around the world, their utilization in nanomaterial synthesis might affect the food chain. To date, a wide range of tea beverages (black, oolong, yellow, green and white tea) are available, which are traditionally produced only from the young tea leaves (bud, first and second leaf). This is achieved *via* a pruning process - a maintaining process in tea plantation to remove the plant branches, matured leaves and roots, which is mandatory to protect the tea plant from diseases. During the pruning process, the matured tea leaves (mother leaf) are considered as waste material. It is worth mentioning that nearly one third of tea plantation is not suitable for drinking or beverage usage and falls into land fill. Thus, we attempt to explore the utilization of waste tea leaves as an economic and recyclable bio-surfactant for CdS QDs synthesis without affecting food chain.

In this work, we demonstrate the biomanufacturing of CdS QDs *via* utilizing the waste mother tea leaves instead of young leaves and explore their anticancer properties against breast cancer cell line.

2. Experimental section

2.1 CdS QDs synthesis using tea leaves

Tea leaves were collected from United Planters Association of Southern India (UPASI), Valparai, Tamil Nadu, India. The mother leaves were separated and washed with distilled H_2O. Leaf samples were chopped and mixed with methanol in 1:10 ratio. The residues in the leaf extract were removed by Whatman filter. The known amount of resultant plant extract was taken, in that 2 mL of aqueous 0.25 M $CdSO_4$ and Na_2S was added and kept under the dark condition for 24 hr incubation to produce CdS QDs [34]. The final CdS QDs solution looks like greenish

yellow color and was subjected to centrifugation. The collected CdS solid pellet was lyophilized. Hereafter, the mother tea leaf mediated CdS QDs will be coined as MT-CdS QDs.

2.2 Characterization of MT-CdS QDs

The as-synthesized MT-CdS QDs were further characterized as followed: (a) FTIR spectral analysis (Shimadzu), with a resolution of 1 cm^{-1} was studied to elucidate the mechanism of action for nanoparticle synthesis. The crystallite structure of as-synthesized MT-CdS QDs was examined using Rigaku D/Max Ultima II powder X-ray diffractometer. Morphology and elemental analysis of lyophilized MT-CdS QDs was analyzed using a HRTEM. Typically, the sonicated samples were coated on the copper TEM grid, and the images of MT-CdS QDs were studied using a FEI Technai F20. The UV-vis absorption and fluorescence emission spectra were performed on a PerkinElmer Lambda 9 and a Horiba FluoroMax-4, respectively. For optical measurements, the MT-CdS QDs were dissolved in ethanol.

2.3 Cytotoxicity assay

MCF-7 cells were purchased from NCCS (National center for cell sciences), Pune and maintained in DMEM medium, supplemented with non-essential amino acids. Cells were maintained at 37ºC in a humidified atmosphere containing 5 % CO_2 in the incubator. Cells were seeded in 96 well culture plates at 2.5×10^3 cells per well for 24 hours. MCF-7 cells were treated with different concentrations (10, 20, 30, 40 and 50 µg/mL) of MT-CdS QDs and kept for 24 h incubation. Then cell viability was examined by MTT (3-(4,5-dimethylthiazol-2-yl)-2,5-diphenyltetrazolium bromide) assay. After 4 hours incubation purple color formazan crystals were formed while adding 100 µl of DMSO and reading was taken at 620 nm in a multi-well ELISA plate reader [35]. The percentage of cell viability was estimated using the formula:

$$\text{Cell viability (\%)} = \frac{\text{OD value of the experiment sample (CdS QDs treated)}}{\text{OD value of the experiment control (Untreated)}} \times 100$$

2.4 Morphological observation

To assess the morphological changes, the MT-CdS QDs treated MCF-7 cells was observed using bright field microscopy. The cells were treated with different concentrations of MT-CdS QDs (15, 30 and 45 µg/mL) and were grown on coverslip for 24 h. They were fixed with methanol and acetic acid solution (3:1, v/v). Then the coverslip was gently mounted on the glass slide. For morphological analysis, the glass slides were viewed under bright field inverted microscope (Nikon) at 40× magnification.

2.5 Fluorescence microscopy study (Apoptosis assessment)

MCF-7 cells were seeded in a 6-well plate and treated with different concentrations (15, 30 and 45 µg/mL) of MT-CdS QDs for 24 h. The treated cells were centrifuged and were washed with PBS (pH 7.2). Finally, cells were stained with 200 µL of AO/EtBr [100 mg/mL of AO (acridine orange) and 100 mg/mL of EtBr (Ethidium Bromide)]. After the cells were incubated for 2 min, the stained cells were visualized under fluorescent microscope at 40× magnification with an excitation filter 480 nm. Similar procedure was followed for DAPI and Annexin V/FITC.

2.6 Cell cycle analysis and Apoptotic analysis by Flow cytometry

MCF-7 cells (1×10^5) were seeded in a six well plate and treated with MT-CdS QDs at different concentrations (15, 30 and 45 µg/mL). After 24 h incubation, both the treated and untreated cells were harvested using trypsin. Then the cells were washed with PBS and stored at -20 $^{\circ}$C for 1 hour, following which the cells were suspended in 0.5 mL of PBS containing 50µg/mL of propidium iodide and 100 µg/mL of RNase. Finally, the cells were incubated at 37°

C for 30 min and were analyzed in BD FACS flow cytometer. Fluorescence signal intensity was recorded and analyzed by Cell Quest and Modifit. To analyze the apoptotic effect, MCF-7 cells were treated with MT-CdS QDs and stained with Annexin V/FITC and propidium iodide and examined using flow cytometry method. After 24 h incubation treated cells were harvested and washed with PBS, and it was treated with Trypsin/EDTA solution. Finally, in the cell pellet 100 µL of Annexin V/FITC and PI (Strong Biotech Co) staining solution was added and incubated for 15 min at 25°C. These stained cells were analyzed with BD FACS flow cytometer.

2.7 Western blot analysis

Western blotting was analyzed to detect the apoptotic and anti-apoptotic proteins of Bcl-2, p53, caspase-3 and Bax. MCF-7 (1×10^5) cells were seeded on to 100 mm culture dishes and the cells were treated with MT-CdS QDs for 24 hours. Then the medium was harvested, and the cells were washed several times with ice cold PBS (pH 7.2). Consequently, the supernatant was removed, and the cells were lysed with lysis buffer (50 mM Tris-Hcl, 150 mM Nacl, 1% Triton X-100, 1 mM phenyl methyl, sulfonyl fluoride, 10 µg/ml pepstatin and 10 µg/ml leuptin) for 20 min. The cells were subjected to centrifugation at 12,000 rpm for 10 min at 4ºC and then supernatant was collected and stored at -80ºC. The collected protein sample concentration was measured using a protein assay kit. The same amount of protein from each sample was applied to 12 % SDS polyacrylamide gel electrophoresis. Then proteins were transferred onto a nitrocellulose membrane and it was blocked for 1 h using 10% skimmed milk in water. The membranes were washed three times with PBS containing 0.1% Tween 20, the primary antibodies (Bcl-2, p53, caspase-3 and Bax) were added at a v/v ratio of 1:1000 and it was incubated overnight at 4ºC. After incubation, the primary antibodies were washed away and secondary antibodies were added for 1 hour incubation at room temperature [36].

2.8 Statistical analysis

All the *in vitro* experiments were carried out in triplicate and the experiments repeated at least three times. Statistical analysis was performed by one-way ANOVA (GraphPad Prism 5.0 software), followed with Bonferroni test for multiple comparisons. Statistical evaluation is performed using the results from a mean standard deviation of three experiments in each batch.

3. Results and discussion

3.1 Structure and morphology analysis

Figure 1(a) shows the XRD result of MT-CdS QDs. The predominent peak exhibits centred around 26.7° corresponds to (111) plane of CdS cubic crystal structure (JCPDS-800019). The broadening amorphous peak shows between 41- 52° due to overlapping (220) and (311) crystalline planes. These broadening nature of crystalline peak indicates the particle size of MT-CdS might be lies in nano regime.

Further, size and morphology of the MT-CdS QDs samples were analyzed using HR-TEM [**Figure 1 (b) and (c)**]. Figure 1(b) shows large number of spherical CdS particles [**Figure 1 (b)-(c)**] those are homogenously dispersed. The particle size of CdS lies between 2 to 4 nm ensuring the QDs formation (<10 nm particle size) which is attributed to the particle size reduction effect by waste tea leaf bio-surfactant. The lattice diameter of CdS QDs were estimated to be 0.33 nm (**Figure 1c**), which implies (111) crystalline phase of cubic CdS. This is inline with XRD results and endorse the CdS crystallite formation through tea leaf extract.

Similar crystalline nature and particle shape was oberved in *E.coli* as green surfactant mediated CdS QDs [37]. Furthermore, the observed elements Cd and S from energy dispersive

spectra (**Figure 1d**) ensure the formation of CdS QDs. It is noteworthy to mention that it is highly challenging to obtain such as smaller particle size *via* the traditional chemical synthesis process at room temperature [38]. This shows that waste tea leaves based green synthesis route is highly promising for producing CdS QDs at room temperature.

3.2 FTIR spectroscopic analysis

FTIR spectra was used to analyze the structural information of the molecules bound on the surface of as-synthesized MT-CdS QDs. The FTIR spectrum of both tea leaf extract and MT-CdS QDs are presented in **Figure 2 (a)** and **(b)**, respectively. **Figure 2 (a)** and **(b)** showed a broad peak around 3600-300 cm^{-1} and 3500-3200 cm^{-1}, which can be assigned to the typical O-H stretching vibration of alcohols and phenols. It is worth mentioning that the N-H stretching vibration bands (3500-3300 cm^{-1}) of the tea leaf extract were not visible, which could be because it was occupied by a strong and large band of carboxyl group in the range [39] . A distinct sharp peak was observed in MT-CdS QDs sample at 2922 cm^{-1} due to C-H stretching that is assigned as anti-symmetric and symmetric ($-CH_2$) vibrations of the hydrocarbon presence in the plant derived protein [25]. The significant peak observed at 1579 and 1042 cm^{-1} corresponds to the amide I (C=O) and amide II (N-H) of the polyphenols or proteins respectively [40]. A weak peak around 617 cm^{-1} is observed in MT-CdS QDs samples attests the existence of the vibrations related to the metal sulfides, confirming the formation of CdS QDs [41, 42]. Through the FTIR spectrum we have confirmed the phytochemicals (polyphenols, caffeine, vitamins, minerals and amino acids) from the tea leaves played major role in the production as well as in the stabilization of CdS QDs. Although the polyphenol content in mother leaves is less than the young tea leaves, it is proven that the matured mother tea leaves exhibits their strong potential in green CdS QDs synthesis. These results are significant, as it corroborates the ability of waste tea

leaves to act as bio-surfactant in CdS QDs synthesis, which would open up new avenues towards manufacturing commodity value products from waste.

3.3 Optical analysis

Figure 3(a) and **(b)** shows the absorption and fluorescence emission spectra of MT-CdS QDs. From Figure 3(a), two band edge shoulders were observed around 410 and 664 nm, thought to be from the absorption edge of CdS and chlorophyll residues from the tea leaf extract, respectively. The corresponding band edge of the CdS peak is 3.03 eV which implies significant blue shift exists for MT-CdS QDs compared to bulk CdS (2.5 eV) [43]. This effect might be due to strong quantum confinement effect through particle size reduction into nano regime as observed in the TEM image. **Figure 3b** shows MT-CdS QDs exhibits strong fluorescence emission around 670 nm. This indicates that the quantum confinement effect exists in MT-CdS QDs as fluorescence emission property strongly rely on their particle size[44]. We have ensured that CdS nanoparticles without tea leaf surfactant does not exhibit the fluorescence property (data not presented in this work). This implies that the tea leaf surfactant predominantly reduces the CdS particle size which brings strong quantum confinement effect and is responsible for fluorescence emission. It is expected that the charge quenching between chlorophyll pigments protein (photosystem II) of tea leaf and CdS QDs interfaces can also facilitate the fluorescence emission[45]. However, a detailed charge transfers investigation on tea leaf extract and MT-CdS QDs using high resolution laser spectroscopy will provide the underlying mechanism of fluorescence emission. The inset of **Figure 3b** showed the photograph of fluorescence emission from MT-CdS QDs solution under UV torch light.

3.4 Cytotoxicity analysis

The cytotoxicity effect of MT-CdS QDs against MCF-7 cell line was evaluated using MTT assay. The growth inhibition was estimated for MT-CdS QDs and compared with the standard drug cisplatin over 24 h. **Figure 4(e)** shows that MT-CdS QDs exhibits dose dependent potential to induced cell death in MCF-7 cells and the performance is comparable with standard drug Cisplatin. The standard drug cisplatin and MT-CdS QDs induced growth inhibiting concentration (IC_{50}) is found to be 15 μg/mL and 30 μg/mL, respectively.

Furthermore, the morphological features of MT-CdS QDs treated MCF-7 cells were examined using bright field inverted microscope. **Figure 4a-d** clearly implies that the MT-CdS QDs treated MCF-7 cells show significant proliferation inhibition compared to untreated cells. The untreated (**Figure 4a**) cells showed an appearance of healthy cytoskeleton structure. On the other hand, the MT-CdS QDs treated cells (**Figure 4b-d**) exhibit irregular shape, cell shrinkage and membrane blebbing with round shape indicating the cell death. The degree of deformation increased with an increase in the MT-CdS QDs dosage. Moreover, it is observed that the MT-CdS QDs treatment induces cell death in MCF-7 cells within 24h. This might be due to the cytotoxicity effect of Cd^{2+} ions and tea leaf polyphenols.

The influence of Cd^{2+} ions on cell death will be explaining in following discussion. At cellular level cadmium species could affects cell proliferation, differentiation, apoptosis and other cellular activities. The Cd^{2+} ions can induce cancer cell death through reactive oxygen species generation. It is well reported that QDs are producing variety of ROS ($O2^{\cdot -}$, H_2O_2 and $OH^{\cdot}$) which create oxidative stress and affects cellular DNA [46]. Recently, Zhao et al,[47] observed ROS induced apoptosis in CdSe/ZnS QDs treated cancer cells. Similarly, Singh *et al* reported the inference of inducing oxidative stress and cell death in prostate cancer cells by biosurfactant CdS QDs treatment *via* releasing Cd^{2+} ion [48]. Significant research has been explored about the

influence of intrinsic Cd^{2+} ions at cellular DNA using different analytical techniques. For instance, Filali et al. [49]demonstrated the role of intrinsic Cd^{2+} ions on synoviocytes through live stream imaging analysis. They examined anti-proliferative effect of CdTe QDs and Cd-free carbon QDs in fibroblast-like synoviocytes (FCL) cells. The CdTe QDs treated cells were showed anti-proliferative effect due to induced cell death via apoptosis and autophagy. The absence of anti-proliferative effect at carbon QDs suggested that cell death was induced by Cd^{2+} and not by a so-called "cargo or vehicle effect" of QDs. This augment advocated MT-CdS QDs are served not only drug vehicle also intrinsic cytotoxicity of Cd^{2+} ions play key role in MC7 cell death.

In the present work, observed polyphenols in the tea leaf mediated CdS QDs (**Figure 2**) also can contribute ROS generation to damage cellular DNA. The tea polyphenols consist of catechins, epigallocatechin-3-gallate (EGCG), epigallocatechin (EGC), epicatechin-3-gallate (ECG), and epicatechin (EC) which have antioxidant reaction sites of meta-5,7-dihydroxyl and di- or trihydroxyl groups [50]. It has been reported that anticarcinogenic effect of catechins in different organs in many animal models, and can be oxidized to generate ROS [51, 52]. Several molecular mechanisms have been suggested for the anticarcinogenic effects of EGCG[53]. Therefore, the tea polyphenols are anticipated to kill the cancer cell in associate with Cd^{2+} ions from QDs. Wide reports explored that tea polyphenols synergistically promote the anticancer activity of other chemotherapy drugs, such as Cisplatin [54], Tamoxifen, and etc [55]. This combinatorial effect has decreased proliferation and induced apoptosis in breast cancer cells. Furthermore, tea polyphenols can minimize or slow the development of drug resistance, as well as reduce drug toxicity and improve therapeutic efficacy [56]. Similarly, it is anticipated that tea polyphenols synergistically promote cytotoxicity effect of CdS QDs on MCF-7 cell damage as is

seen in **Figure 4 (b-d)**. However, further experimental investigation is needed to ensure the apoptosis induced cell death and mitochondria dysfunction by MT-CdS QDs.

3.5 Fluorescence microscope analysis

In order to study the cytotoxic effect of MT-CdS QDs at cellular DNA we carried out fluorescence staining analysis. AO/EB staining is used for evaluate the induction of apoptosis and necrosis [57]. The nuclear fragmentation and apoptotic bodies detection were examined at MFC-7 cell line using DAPI and Annexin V/FiTC staining. The corresponding results of each staining are discussed in the following session.

In order to study the apoptosis mechanism, the MCF-7 cells were treated with MT-CdS QDs for 24 h and were assessed by fluorescence microscopy using AO/EtBr (Acridine Orange and Ethidium Bromide) staining. AO is a green fluorescence emitting dye that can penetrate the normal cell membrane. The Ethidium Bromide emits red fluorescence upon binding with non-viable cells due to loss of their membrane integrity. Early and late apoptotic cells are highlights in green and bright orange fragmented condensed nuclei [35]. The **Figure 5 a-d** shows the AO/EB staining results of untreated and MT-CdS QDs treated MCF-7 cells. From Figure 5a-d observed orange color indicates different characteristics of apoptotic bodies such as cell shrinkage, nuclear condensation and fragmented nuclei. Furthermore, this effect has been gradually increased with increasing QDs ensures the influence of MT-CdS QDs on apoptosis effect.

Further, hallmark of the apoptosis is confirmed by DNA fragmentation process using DAPI staining analysis. The DAPI is a blue fluorescent DNA stain usually it emits higher fluorescence

while binding with double stranded DNA with a preference of adenine and thymine clusters. In the resulting, apoptotic nucleus indicates with the higher fluorescence emission [58]. The DAPI staining results of untreated and MT-CdS QDs treated MCF-7 cells are presented in **Figure 5e** and **Figure 5 (f-h)**, respectively. The untreated (**Figure 5e**) MCF-7 cells show normal morphology with intact round nucleus which emits weak fluorescence. In the case of MT-CdS QDs treated cells results strong fluorescence (**Figure 5f-h**) which ensures existence of apoptotic nuclei and nuclear condensation. As is explained in 3.4, the ROS generation by tea polyphenols and Cd^{2+} ions are results double stranded DNA breakage or DNA damage is the reason for apoptosis induced cell death [59]. Similar nuclei fragmentation was noticed at Hela cells treated with doxorubicin drug conjugated nanoparticles [60].

Annexin V-FITC staining was used to qualitatively study the apoptotic stage at MCF-7 cells. In live cells phosphatidylserine (PS) an anionic phospholipid, is actively translocated to the inner leaflet of the cell membrane. During the apoptosis process, the PS cells distribution is randomized and appeared on outer leaflet of the cell membrane. Therefore, the detection of phosphatidylserine indicates the apoptosis process induced cell death. Typically, Annexin V-FITC (anticoagulant protein) stain is conjugated with fluorochrome which preferentially binds with PS. If Annexin V-FITC stain emitting green fluorescence indicates live bodies whereas red fluorescence implies apoptotic bodies. The fluorescence images of Annexin V-FITC stained untreated MCF-7 cells (**Figure 5(i)**) shows only the green emission, confirming the live cells. However, as anticipated, red emission is observed in the fluorescence images (**Figure 5(j-l)**) of the MCF-7 cell samples treated with various dosages of MT-CdS QDs indicating that the existence of apoptosis process as a result of MT-CdS QDs treatment. Also, the density of red spots increased with an increase in the MT-CdS QDs dosage implies the capability of MT-CdS

QDs to induce effective cell death. Therefore, these results ensured MT-CdS QDs are strongly producing apoptosis induced cell death at MCF-7 cells and is in line with cytotoxic results (**Figure 4b-d**).

3.6 Cell cycle analysis and apoptosis assessment

To explore the mechanism of anticancer effect induced by MT-CdS QDs in MCF-7 cells, cell cycle distribution was assessed by flow cytometry analysis (FACS). **Figure 6** displays the FACS results. From **Figure 6**, it is observed that the cell count of MT-CdS QDs treated cells are significantly reduced at S phase (27.83, 21.65 and 18.43 %) as well as G_2/M phase (23.12, 21.73 and 19.2 %) over time. By increasing the dosage from 15 to 45 µg/mL, the cell death is found to increase gradually. Overall, the cell death rate is high at MT-CdS QDs treated cell compared to untreated cells (**Figure 6e**). It is clearly demonstrated that the cell cycle was arrested at S phase and G2/M phase. As previously discussed in cytotoxicity and fluorescence analysis session, cell cycle arrest might be due to Cd^{2+} ions induced mitochondrial dysfunction and DNA damage at S phase which induces the cell death [61]. In the case of untreated cell, the untreated cells (**Figure 6a**) are showing progression stage and it has dividing capability for multiplication. Similar observations were reported by Sui *et al.* [10] on graphene QDs treated MCF-7 cells as well as the iron oxide nanoparticle treated MDA-MB-231 (breast cancer) cells without any drug conjugation [61]. It implies that semiconductor QDs synthesized from waste tea leaf can effectively induce the apoptosis process like chemically synthesized nanoparticle.

Further, exclusively detect apoptotic and necrotic cells, the Annexin V/FITC and PI was used in flow cytometry analysis. The results were summarized in **Figure 7 (a)-(d)**. The induction of apoptosis was determined based on the cells falls in the quadrants. From **Figure 7 (a)-(d)**,

upper left quadrant indicated necrotic cells, and upper right quadrant represents late apoptotic cells. The lower right and left quadrant indicates early apoptotic and live cells, respectively. Over all, the existence of apoptotic cells was observed only in the MT-CdS QDs treated MCF-7 cells and no apoptotic cells were observed in untreated cells. The quantitative results of apoptosis assessment were summarized in **Figure 7e**. These results clearly imply that MT-CdS QDs induces apoptosis in MCF-7 cells at 24 h incubation time.

3.7 Western blot analysis

In order to dechiper the molecular mechanism involved in the apoptosis of MT-CdS QDs induced breast cancer cells western blot analysis was carried out. In this study, the expression profile of apoptotic and anti-apoptotic proteins Bax, p53, caspase-3 and Bcl-2 proteins, respetively were analyzed. The house keeping gene β-actin was used as a internal control protein in this analysis. The **Figure 8** shows the Bax, p53, caspase-3 are upregulated, and Bcl-2 protein was downregulated. These results sheds light on cell death process observed at MT-CdS QDs treated breast cancer cells. Firstly, down-regulation of Bcl-2 protein indicates the poor cytoprotectivity of MCF-7 cell and fails to inhibit the apoptosis pathway [62]. It is reported that, p53 protein will regulate apoptosis through interaction with the Bcl-2 family, and was confirmed by p53 up-regulation in **Figure 8** [63]. Furthermore, the up-regulation of apoptotic protein Bax in **Figure 8** pointed out the series of structural changes that culminate in the translocation of Bax from the cytosol to the mitochondria outer membrane (MOM). While anchoring Bax with MOM it induces oligomerization process and creates a pore where cytochrome *c* escape and activate the caspase cascade that facilitate apoptosis[64]. The caspase 3 is a cleaving cellular protein essential for cell survival via DNA fragmentation. Through caspase cascade process, the caspase 3 protein induced apoptosis at MCF-7 cells. Therefore, p53 and caspase 3 are responsible for observed cell

cycle arrest at S phase (**Figure 6**) and cytotoxicity effect (**Figure 4**) at MT-CdS QDs treated MCF-7 cells, respectively. Based on the western blot analysis we proposed posssible mechanism of apoptosis process occurred in under MT-CdS QDs trated breast cancer cells in **Scheme 1**. From the above discussion we can summarize that advantageous of tea leaf polyphenols on CdS QDs including (a) CdS particle size reduction, (b) fluorescence emission, and (c) producing ROS. Our previous report [34] showed preliminary results of tea leaf mediated CdS QDs on hemolysis effect. 60 µg/mL of CdS QDs results 1.8% of hemolysis effect in red blood cells was still lower than allowed effect (5%). Though these results encouraging the utilization of tea leaf mediated CdS QDs in cancer theranostics application, however, further research on mice model (*in vivo*) is necessitate to understand selective anti-proliferation effect of tea leaf mediated CdS QDs on producing metal intoxication effect. This may be useful in the development of green synthesized QDs based anti-cancer drugs.

4. Conclusion

In this work, we have successfully demonstrated a simple route for the synthesis of semiconductor QDs using waste tea leaves as a bio-surfactant. The tea polyphenols play a major role in biomanufacturing of QDs production. For instance, we have reported young tea leaves mediated CdS QDs of size ranging from 2 to 5nm with better photoluminescence in our previous study [34]. Though, waste matured tea leaves contain less amount of polyphenols compared to young leaves, our experimental evidence proves that it is sufficient for producing quantum dots. Furthermore, tea polyphenols from tea leave extract and Cd^{2+} ions from CdS QDs synergistically produce ROS which promotes apoptosis in breast cancer via p53, Bcl-2/Bax and caspase-3 mediated pathway. However, it needs further investigation on *in vivo* analysis that might help to understand the apoptosis effect of MT-CdS QDs in animal model. Therefore, it is anticipated that

the utilization of MT-CdS QDs produced from waste tea leaves as bi-functional drug and delivery vehicle in cancer treatment will be a promising approach. Also, this is a simple and circular economic route for producing biocompatible QDs at low-cost, which could simultaneously benefit tea and biomedical industries.

Acknowledgements

The authors KS and MGB thank the Principal and Head, Department of Biotechnology, K.S. Rangasammy College of Technology, Tiruchengode, Tamil Nadu, India for the support offered towards study. These authors also acknowledge DST-FIST (fund for infrastructure) for science and technology (SR/FST/College-235/2014 dated 21.11.2014). S.P. acknowledges Welsh Government and European Regional Development Fund (ERDF) for supporting Rising Star Fellowship. A.D acknowledges Ser Cymru II MSCA COFUND Fellowship jointly funded by Welsh Government and European Commission through ERDF funds. MLD and CD are grateful for the financial support of the EPSRC (EP/R016666/1 and EP/S001336/1) and both the EPSRC and Innovate UK for the SPECIFIC Innovation and Knowledge Centre and for the support from the European Regional Development Fund through the Welsh Government to the Sêr Solar program. All authors thank to Kanan Devan Hills plantations company (p) ltd, Munnar, Kerala, for their constant support.

References

[1] N. Chen, Y. He, Y. Su, X. Li, Q. Huang, H. Wang, X. Zhang, R. Tai, C. Fan, The cytotoxicity of cadmium-based quantum dots, Biomaterials, 33 (2012) 1238-1244.

[2] Y.N. Wu, L.X. Yang, X.Y. Shi, I.C. Li, J.M. Biazik, K.R. Ratinac, D.H. Chen, P. Thordarson, D.B. Shieh, F. Braet, The selective growth inhibition of oral cancer by iron core-gold shell nanoparticles through mitochondria-mediated autophagy, Biomaterials, 32 (2011) 4565-4573.

[3] M. Ahamed, M.J. Akhtar, M. Raja, I. Ahmad, M.K. Siddiqui, M.S. AlSalhi, S.A. Alrokayan, ZnO nanorod-induced apoptosis in human alveolar adenocarcinoma cells via p53, survivin and bax/bcl-2 pathways: role of oxidative stress, Nanomedicine : nanotechnology, biology, and medicine, 7 (2011) 904-913.

[4] M.I. Khan, A. Mohammad, G. Patil, S.A. Naqvi, L.K. Chauhan, I. Ahmad, Induction of ROS, mitochondrial damage and autophagy in lung epithelial cancer cells by iron oxide nanoparticles, Biomaterials, 33 (2012) 1477-1488.

[5] A.M. Derfus, W.C.W. Chan, S.N. Bhatia, Probing the Cytotoxicity of Semiconductor Quantum Dots, Nano Letters, 4 (2004) 11-18.

[6] R. Singh, H.S. Nalwa, Medical applications of nanoparticles in biological imaging, cell labeling, antimicrobial agents, and anticancer nanodrugs, Journal of biomedical nanotechnology, 7 (2011) 489-503.

[7] J. Ruan, H. Song, Q. Qian, C. Li, K. Wang, C. Bao, D. Cui, HER2 monoclonal antibody conjugated RNase-A-associated CdTe quantum dots for targeted imaging and therapy of gastric cancer, Biomaterials, 33 (2012) 7093-7102.

[8] M. Fang, C.-W. Peng, D.-W. Pang, Y. Li, Quantum dots for cancer research: current status, remaining issues, and future perspectives, Cancer biology & medicine, 9 (2012) 151-163.

[9] K.-T. Yong, R. Hu, I. Roy, H. Ding, L.A. Vathy, E.J. Bergey, M. Mizuma, A. Maitra, P.N. Prasad, Tumor targeting and imaging in live animals with functionalized semiconductor quantum rods, ACS applied materials & interfaces, 1 (2009) 710-719.

[10] X. Sui, C. Luo, C. Wang, F. Zhang, J. Zhang, S. Guo, Graphene quantum dots enhance anticancer activity of cisplatin via increasing its cellular and nuclear uptake, Nanomedicine : nanotechnology, biology, and medicine, 12 (2016) 1997-2006.

[11] K.G. Li, J.T. Chen, S.S. Bai, X. Wen, S.Y. Song, Q. Yu, J. Li, Y.Q. Wang, Intracellular oxidative stress and cadmium ions release induce cytotoxicity of unmodified cadmium sulfide quantum dots, Toxicology in vitro : an international journal published in association with BIBRA, 23 (2009) 1007-1013.

[12] Y. Li, W. Lu, Q. Huang, M. Huang, C. Li, W. Chen, Copper sulfide nanoparticles for photothermal ablation of tumor cells, Nanomedicine (London, England), 5 (2010) 1161-1171.

[13] M.P. Melancon, M. Zhou, C. Li, Cancer theranostics with near-infrared light-activatable multimodal nanoparticles, Acc Chem Res, 44 (2011) 947-956.

[14] D. Fragouli, A.M. Laera, G. Caputo, V. Resta, P.P. Pompa, L. Tapfer, R. Cingolani, A. Athanassiou, The effect of polymer matrices in the in-situ cds formation under uv irradiation of precursor-polymer films, 2018.

[15] F. Di Benedetto, A. Camposeo, L. Persano, A.M. Laera, E. Piscopiello, R. Cingolani, L. Tapfer, D. Pisignano, Light-emitting nanocomposite CdS-polymer electrospun fibres via in situ nanoparticle generation, Nanoscale, 3 (2011) 4234-4239.

[16] Y. Zou, D. Li, D. Yang, Shape and phase control of CdS nanocrystals using cationic surfactant in noninjection synthesis, Nanoscale Research Letters, 6 (2011) 374.

[17] F. Osaki, T. Kanamori, S. Sando, T. Sera, Y. Aoyama, A Quantum Dot Conjugated Sugar Ball and Its Cellular Uptake. On the Size Effects of Endocytosis in the Subviral Region, Journal of the American Chemical Society, 126 (2004) 6520-6521.

[18] J.A. Champion, S. Mitragotri, Role of target geometry in phagocytosis, Proceedings of the National Academy of Sciences of the United States of America, 103 (2006) 4930-4934.

[19] Y. Geng, P. Dalhaimer, S. Cai, R. Tsai, M. Tewari, T. Minko, D.E. Discher, Shape effects of filaments versus spherical particles in flow and drug delivery, Nat Nanotechnol, 2 (2007) 249-255.

[20] F. Erogbogbo, K.-T. Yong, I. Roy, G. Xu, P.N. Prasad, M.T. Swihart, Biocompatible Luminescent Silicon Quantum Dots for Imaging of Cancer Cells, ACS nano, 2 (2008) 873-878.

[21] K.E. Sapsford, W.R. Algar, L. Berti, K.B. Gemmill, B.J. Casey, E. Oh, M.H. Stewart, I.L. Medintz, Functionalizing Nanoparticles with Biological Molecules: Developing Chemistries that Facilitate Nanotechnology, Chemical Reviews, 113 (2013) 1904-2074.

[22] V. Biju, Chemical modifications and bioconjugate reactions of nanomaterials for sensing, imaging, drug delivery and therapy, Chemical Society Reviews, 43 (2014) 744-764.

[23] N. Erathodiyil, J.Y. Ying, Functionalization of Inorganic Nanoparticles for Bioimaging Applications, Accounts of Chemical Research, 44 (2011) 925-935.

[24] M. Divya Rao, G. Pennathur, Green synthesis and characterization of cadmium sulphide nanoparticles from Chlamydomonas reinhardtii and their application as photocatalysts, 2017.

[25] G. Chen, B. Yi, G. Zeng, Q. Niu, M. Yan, A. Chen, J. Du, J. Huang, Q. Zhang, Facile green extracellular biosynthesis of CdS quantum dots by white rot fungus Phanerochaete chrysosporium, Colloids and surfaces. B, Biointerfaces, 117 (2014) 199-205.

[26] M. Borovaya, Y. Pirko, T. Krupodorova, A. Naumenko, Y. Blume, A. Yemets, Biosynthesis of cadmium sulphide quantum dots by using Pleurotus ostreatus (Jacq.) P. Kumm, Biotechnology & Biotechnological Equipment, 29 (2015) 1156-1163.

[27] C. Mi, Y. Wang, J. Zhang, H. Huang, L. Xu, S. Wang, X. Fang, J. Fang, C. Mao, S. Xu, Biosynthesis and characterization of CdS quantum dots in genetically engineered Escherichia coli, J Biotechnol, 153 (2011) 125-132.

[28] M.R. Kim, D. Ma, Quantum-Dot-Based Solar Cells: Recent Advances, Strategies, and Challenges, The Journal of Physical Chemistry Letters, 6 (2015) 85-99.

[29] C.-H.M. Chuang, A. Maurano, R.E. Brandt, G.W. Hwang, J. Jean, T. Buonassisi, V. Bulović, M.G. Bawendi, Open-Circuit Voltage Deficit, Radiative Sub-Bandgap States, and Prospects in Quantum Dot Solar Cells, Nano letters, 15 (2015) 3286-3294.

[30] Q. Bai, Z. Zhao, H. Sui, J. Chen, X. Xie, F. Wen, The Preparation and Application of Dendrimer Modified CdTe/CdS Near Infrared Quantum Dots for Brain Cancer Cells Imaging, Applied Sciences, 5 (2015) 1076.

[31] H. Yukawa, Y. Baba, In Vivo Fluorescence Imaging and the Diagnosis of Stem Cells Using Quantum Dots for Regenerative Medicine, Analytical Chemistry, 89 (2017) 2671-2681.

[32] A.C.S. Samia, X. Chen, C. Burda, Semiconductor Quantum Dots for Photodynamic Therapy, Journal of the American Chemical Society, 125 (2003) 15736-15737.

[33] B.R. Singh, B.N. Singh, W. Khan, H.B. Singh, A.H. Naqvi, ROS-mediated apoptotic cell death in prostate cancer LNCaP cells induced by biosurfactant stabilized CdS quantum dots, Biomaterials, 33 (2012) 5753-5767.

[34] K. Shivaji, S. Mani, P. Ponmurugan, C.S. De Castro, M. Lloyd Davies, M.G. Balasubramanian, S. Pitchaimuthu, Green-Synthesis-Derived CdS Quantum Dots Using Tea

Leaf Extract: Antimicrobial, Bioimaging, and Therapeutic Applications in Lung Cancer Cells, ACS Applied Nano Materials, 1 (2018) 1683-1693.

[35] R. Vivek, R. Thangam, K. Muthuchelian, P. Gunasekaran, K. Kaveri, S. Kannan, Green biosynthesis of silver nanoparticles from Annona squamosa leaf extract and its in vitro cytotoxic effect on MCF-7 cells, Process Biochemistry, 47 (2012) 2405-2410.

[36] K. Vimala, S. Sundarraj, M.V. Sujitha, S. Kannan, Curtailing Overexpression of E2F3 in Breast Cancer Using siRNA (E2F3)-Based Gene Silencing, Archives of Medical Research, 43 (2012) 415-422.

[37] R.Y. Sweeney, C. Mao, X. Gao, J.L. Burt, A.M. Belcher, G. Georgiou, B.L. Iverson, Bacterial Biosynthesis of Cadmium Sulfide Nanocrystals, Chemistry & Biology, 11 (2004) 1553-1559.

[38] J. Joo, H.B. Na, T. Yu, J.H. Yu, Y.W. Kim, F. Wu, J.Z. Zhang, T. Hyeon, Generalized and Facile Synthesis of Semiconducting Metal Sulfide Nanocrystals, Journal of the American Chemical Society, 125 (2003) 11100-11105.

[39] S.B. Choi, Y.-S. Yun, Biosorption of cadmium by various types of dried sludge: An equilibrium study and investigation of mechanisms, Journal of Hazardous Materials, 138 (2006) 378-383.

[40] Q. Sun, X. Cai, J. Li, M. Zheng, Z. Chen, C.-P. Yu, Green synthesis of silver nanoparticles using tea leaf extract and evaluation of their stability and antibacterial activity, Colloids and Surfaces A: Physicochemical and Engineering Aspects, 444 (2014) 226-231.

[41] G. Murugadoss, R. Thangamuthu, R. Jayavel, M. Rajesh Kumar, Narrow with tunable optical band gap of CdS based core shell nanoparticles: Applications in pollutant degradation and solar cells, Journal of Luminescence, 165 (2015) 30-39.

[42] T.P. Martin, H. Schaber, Matrix isolated II-VI molecules: Sulfides of Mg, Ca, Sr, Zn and Cd, Spectrochimica Acta Part A: Molecular Spectroscopy, 38 (1982) 655-660.

[43] H. Cao, G. Wang, S. Zhang, X. Zhang, D. Rabinovich, Growth and Optical Properties of Wurtzite-Type CdS Nanocrystals, Inorganic Chemistry, 45 (2006) 5103-5108.

[44] A. Ben Moshe, D. Szwarcman, G. Markovich, Size Dependence of Chiroptical Activity in Colloidal Quantum Dots, ACS Nano, 5 (2011) 9034-9043.

[45] E.H. Murchie, T. Lawson, Chlorophyll fluorescence analysis: a guide to good practice and understanding some new applications, Journal of Experimental Botany, 64 (2013) 3983-3998.

[46] G. Bertin, D. Averbeck, Cadmium: cellular effects, modifications of biomolecules, modulation of DNA repair and genotoxic consequences (a review), Biochimie, 88 (2006) 1549-1559.

[47] M.-X. Zhao, B.-J. Zhu, W.-J. Yao, D.-F. Chen, Therapeutic effect of quantum dots for cancer treatment, RSC Advances, 6 (2016) 113791-113795.

[48] B.R. Singh, B.N. Singh, W. Khan, H.B. Singh, A.H. Naqvi, ROS-mediated apoptotic cell death in prostate cancer LNCaP cells induced by biosurfactant stabilized CdS quantum dots, Biomaterials, 33 (2012) 5753-5767.

[49] S. Filali, A. Geloën, V. Lysenko, F. Pirot, P. Miossec, Live-stream characterization of cadmium-induced cell death using visible CdTe-QDs, Scientific Reports, 8 (2018) 12614.

[50] S.C. Forester, J.D. Lambert, The role of antioxidant versus pro-oxidant effects of green tea polyphenols in cancer prevention, Molecular nutrition & food research, 55 (2011) 844-854.

[51] H.-S. Kim, M.J. Quon, J.-a. Kim, New insights into the mechanisms of polyphenols beyond antioxidant properties; lessons from the green tea polyphenol, epigallocatechin 3-gallate, Redox Biology, 2 (2014) 187-195.

[52] C.S. Yang, H. Wang, G.X. Li, Z. Yang, F. Guan, H. Jin, Cancer prevention by tea: Evidence from laboratory studies, Pharmacological Research, 64 (2011) 113-122.

[53] C.S. Yang, S. Bian, H. Wang, Green tea polyphenol EGCG suppresses lung cancer cell growth through upregulating miR-210 expression caused by stabilizing HIF-1α, Carcinogenesis, 32 (2011) 1881-1889.

[54] M.M. Chan, D. Fong, K.J. Soprano, W.F. Holmes, H. Heverling, Inhibition of growth and sensitization to cisplatin-mediated killing of ovarian cancer cells by polyphenolic chemopreventive agents, Journal of Cellular Physiology, 194 (2003) 63-70.

[55] M.J. Scandlyn, E.C. Stuart, T.J. Somers-Edgar, A.R. Menzies, R.J. Rosengren, A new role for tamoxifen in oestrogen receptor-negative breast cancer when it is combined with epigallocatechin gallate, British journal of cancer, 99 (2008) 1056-1063.

[56] J. Cao, J. Han, H. Xiao, J. Qiao, M. Han, Effect of Tea Polyphenol Compounds on Anticancer Drugs in Terms of Anti-Tumor Activity, Toxicology, and Pharmacokinetics, Nutrients, 8 (2016) 762.

[57] M. Leite, M. Quinta-Costa, P.S. Leite, J.E. Guimaraes, Critical evaluation of techniques to detect and measure cell death--study in a model of UV radiation of the leukaemic cell line HL60, Analytical cellular pathology : the journal of the European Society for Analytical Cellular Pathology, 19 (1999) 139-151.

[58] B. Chazotte, Labeling nuclear DNA using DAPI, Cold Spring Harbor protocols, 2011 (2011) pdb.prot5556.

[59] K. Shanthi, K. Vimala, D. Gopi, S. Kannan, Fabrication of a pH responsive DOX conjugated PEGylated palladium nanoparticle mediated drug delivery system: an in vitro and in vivo evaluation, RSC Advances, 5 (2015) 44998-45014.

[60] B. Sahoo, K.S. Devi, R. Banerjee, T.K. Maiti, P. Pramanik, D. Dhara, Thermal and pH responsive polymer-tethered multifunctional magnetic nanoparticles for targeted delivery of anticancer drug, ACS applied materials & interfaces, 5 (2013) 3884-3893.

[61] K. Kavithaa, M. Paulpandi, P.R. Padma, S. Sumathi, Induction of intrinsic apoptotic pathway and cell cycle arrest via baicalein loaded iron oxide nanoparticles as a competent nano-mediated system for triple negative breast cancer therapy, RSC Advances, 6 (2016) 64531-64543.

[62] A.S. Pearson, F.R. Spitz, S.G. Swisher, M. Kataoka, M.G. Sarkiss, R.E. Meyn, T.J. McDonnell, R.J. Cristiano, J.A. Roth, Up-Regulation of the Proapoptotic Mediators Bax and Bak after Adenovirus-mediated p53 Gene Transfer in Lung Cancer Cells, Clinical Cancer Research, 6 (2000) 887.

[63] S.K. Chiou, L. Rao, E. White, Bcl-2 blocks p53-dependent apoptosis, Molecular and cellular biology, 14 (1994) 2556-2563.

[64] S. Cory, J.M. Adams, Killing cancer cells by flipping the Bcl-2/Bax switch, Cancer Cell, 8 (2005) 5-6.

Figure Captions

Figure 1. (a) XRD pattern and HR-TEM images of waste tea leaf (*Camellia senensis*) mediated CdS QDs at (b) 20 nm scale and (c) 5 nm scale and (d) energy dispersion spectra of waste tea leaf mediated CdS QDs.

Figure 2. FTIR spectra of (a) waste tea leaf extract (b) waste leaf extract mediated CdS QDs (MT-CdS QDs).

Figure 3. (a) Absorption and (b) Fluorescence (λ_{exc} = 410 nm) emission spectra of MT-CdS QDs in ethanol at room temperature.

Figure 4. High contrast microscope images of (a) untreated and treated MCF-7 cells with MT-CdS QDs at (b) 15 µg/mL, (c) 30 µg/mL and (d) 45 µg/mL over 24 h; (e) comparative plot for % of cell viability in MCF-7 cell line treated with CdS QDs and standard drug (Cisplatin).

Figure 5. Fluorescence microscopy images of (a) untreated MCF-7 cell line, and CdS QDs treated MCF-7 cell line with different concentrations (b) 15 µg/mL (c) 30 µg/mL (d) 45 µg/mL. [Note that AO/EtBr stain is used in these measurements. The live cells appeared in green colour. In the case of early and late apoptotic cells were appeared in yellow and reddish orange]. (e) untreated MCF-7 cells (f) 15 µg/mL (g) 30 µg/mL and (h) 45 µg/mL of CdS QDs treated with MCF-7 cells for 24h, and stained with DAPI. Annexin V/FITC apoptotic analysis of (i) untreated MCF-7 cell line and; CdS QDs treated MCF-7 cell line with different concentrations (j) 15 µg/mL (k) 30 µg/mL (l) 45 µg/mL. The arrow indicates apoptotic cells (red color spots).

Figure 6. Flow cytometry analysis of (a) untreated MCF-7 cell line and; CdS QDs treated MCF-7 cell line with different dose concentrations, (b) 15 µg/mL, (c) 30 µg/mL and (d) 45 µg/mL; (e) estimated cell viability in breast cancer cells using figures (a) – (d).

Figure 7. The apoptotic cell death in MCF-7 cell line analysed by flow cytometry using Annexin –FITC/PI staining (a) untreated and; CdS QDs treated MCF-7 cell line with different concentrations (b) 15 µg/mL (c) 30 µg/mL (d) 45 µg/mL. Note that the fluorescence intensity of Annexin – FITC/PI stained apoptotic cells expressed at the top and bottom right quadrants are in late and early apoptosis, respectively; (e) percentage of live, apoptotic, pro-apoptotic and necrotic cells estimated from untreated and MT-CdS QDs treated MCF-7 cells (note that the cell line is stained with Annexin V/FITC).

Figure 8. Regulation of anti-apoptotic proteins and apoptotic proteins in MCF-7 cell line treated with different concentrations of CdS QDs through western blot technique; (b) the expression of apoptotic and anti-apoptotic proteins estimated from MT-CdS QDs treated MCF-7 cells, and compared with untreated cell.

Scheme.1 Schematic illustration apoptosis process via mitochondrial intrinsic pathway in breast cancer cells under green synthesized CdS QDs treatment.

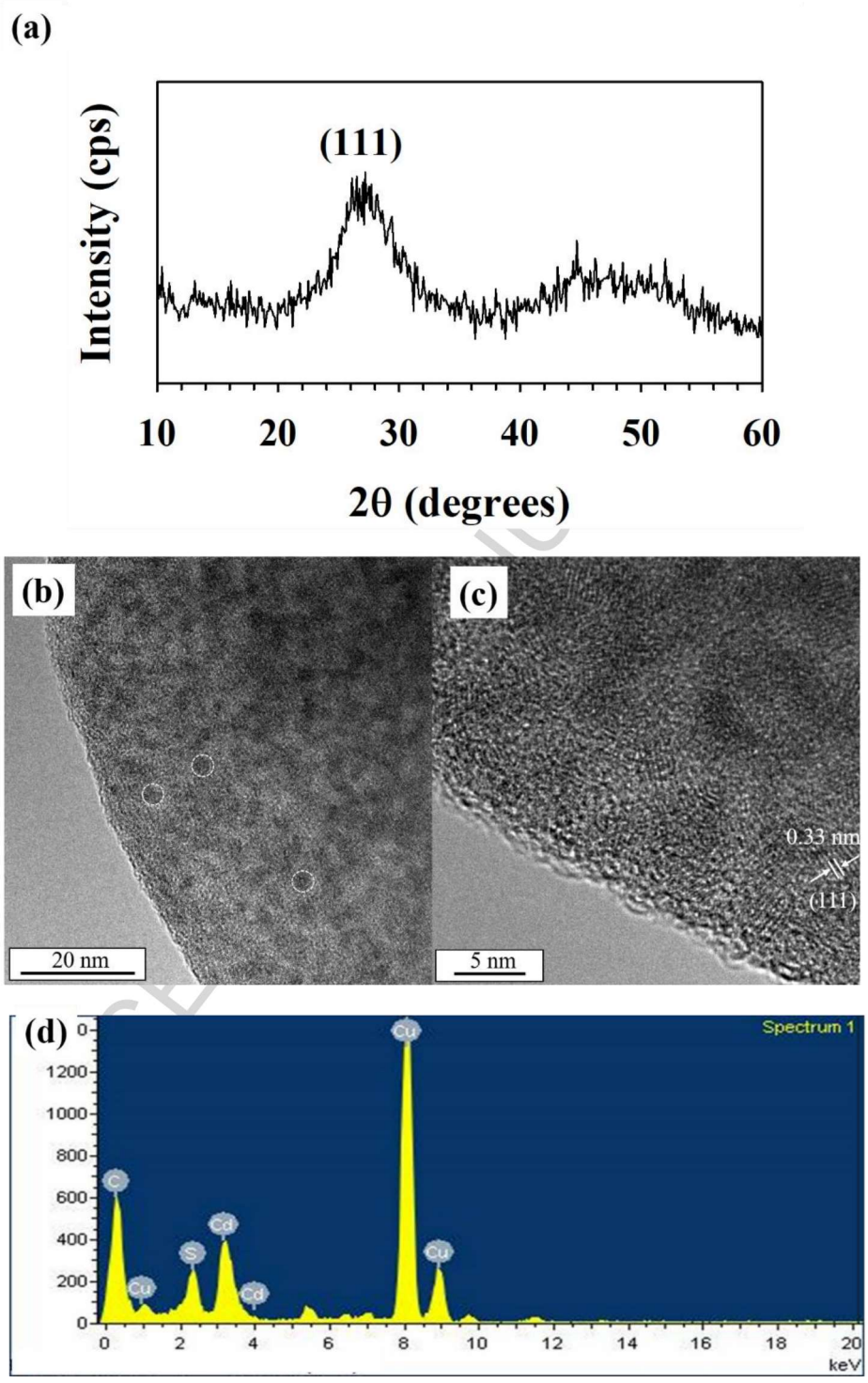

Figure 1.

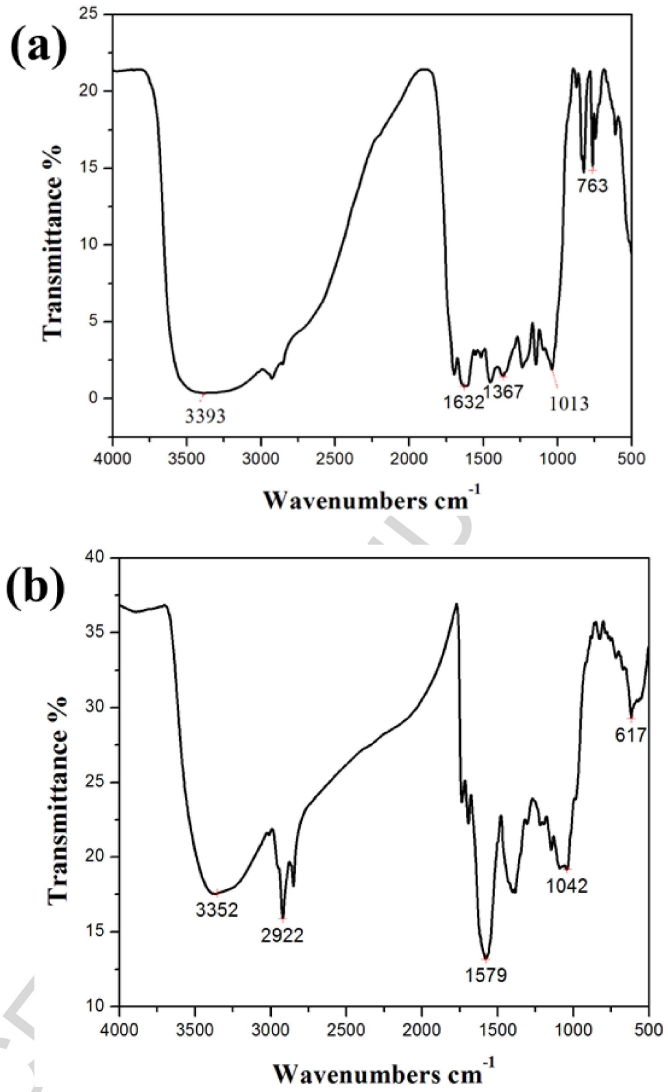

Figure 2.

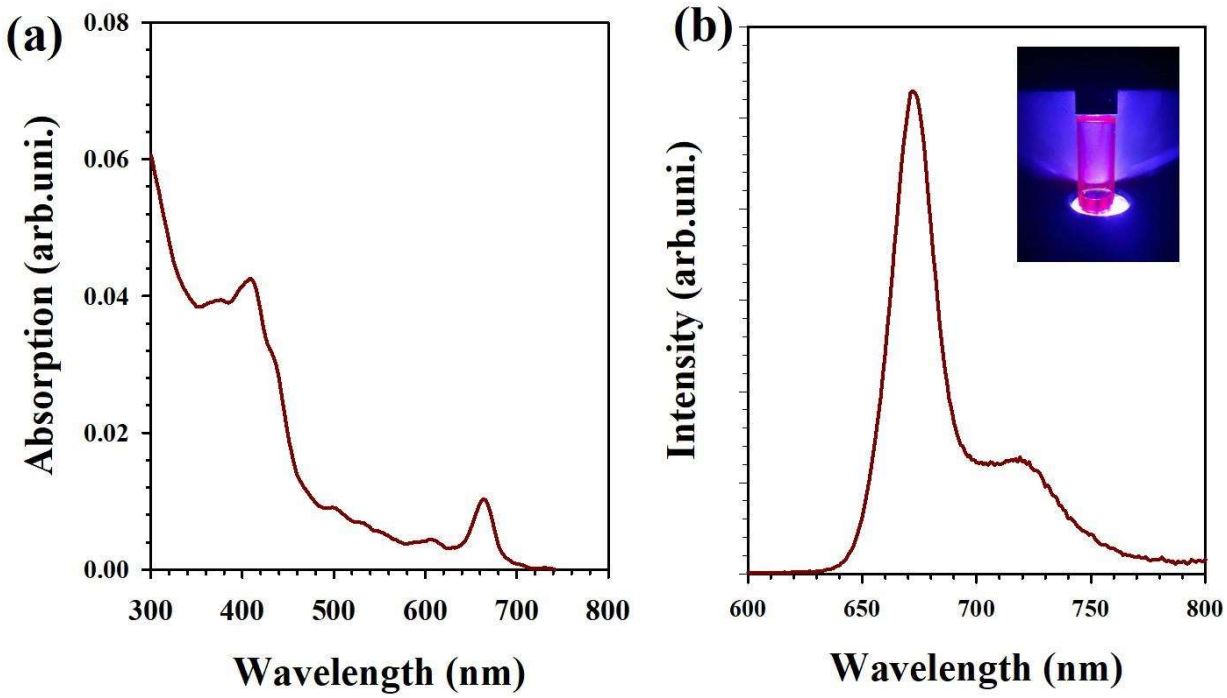

Figure 3.

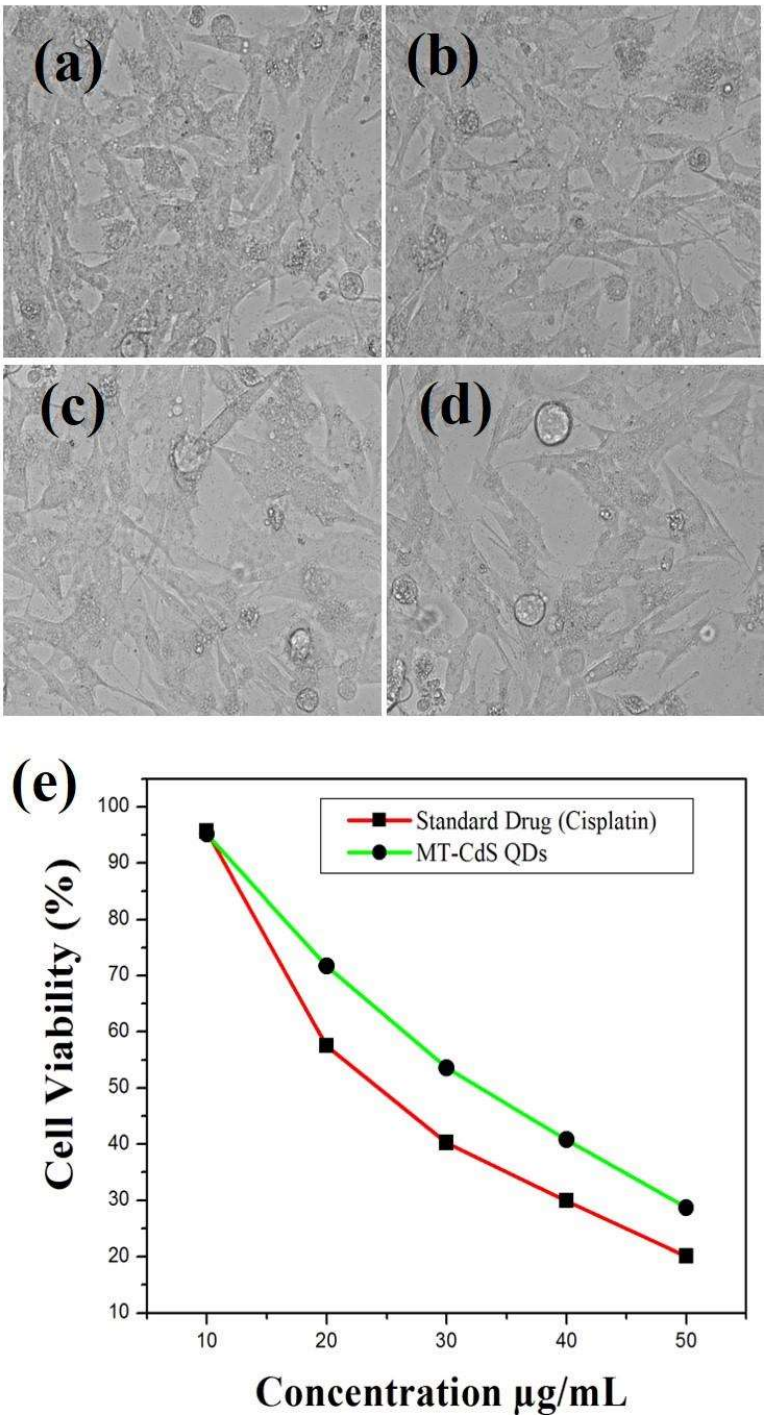

Figure 4.

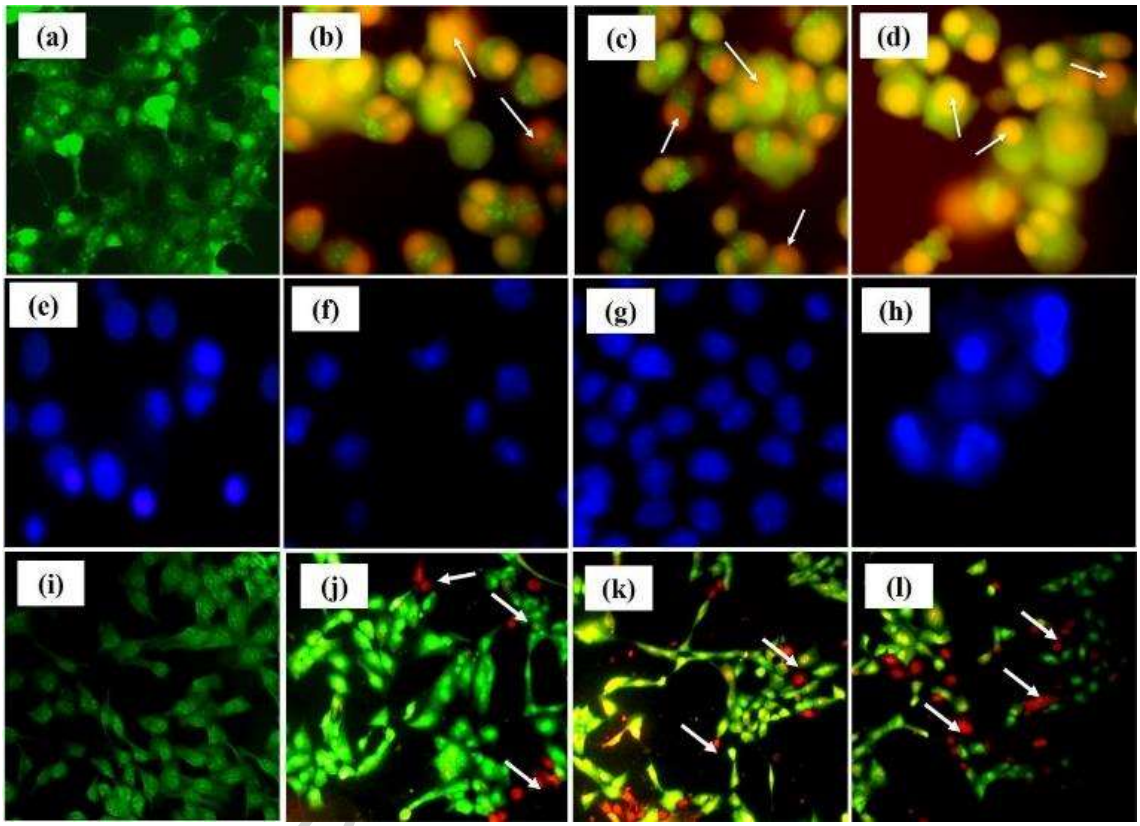

Figure 5.

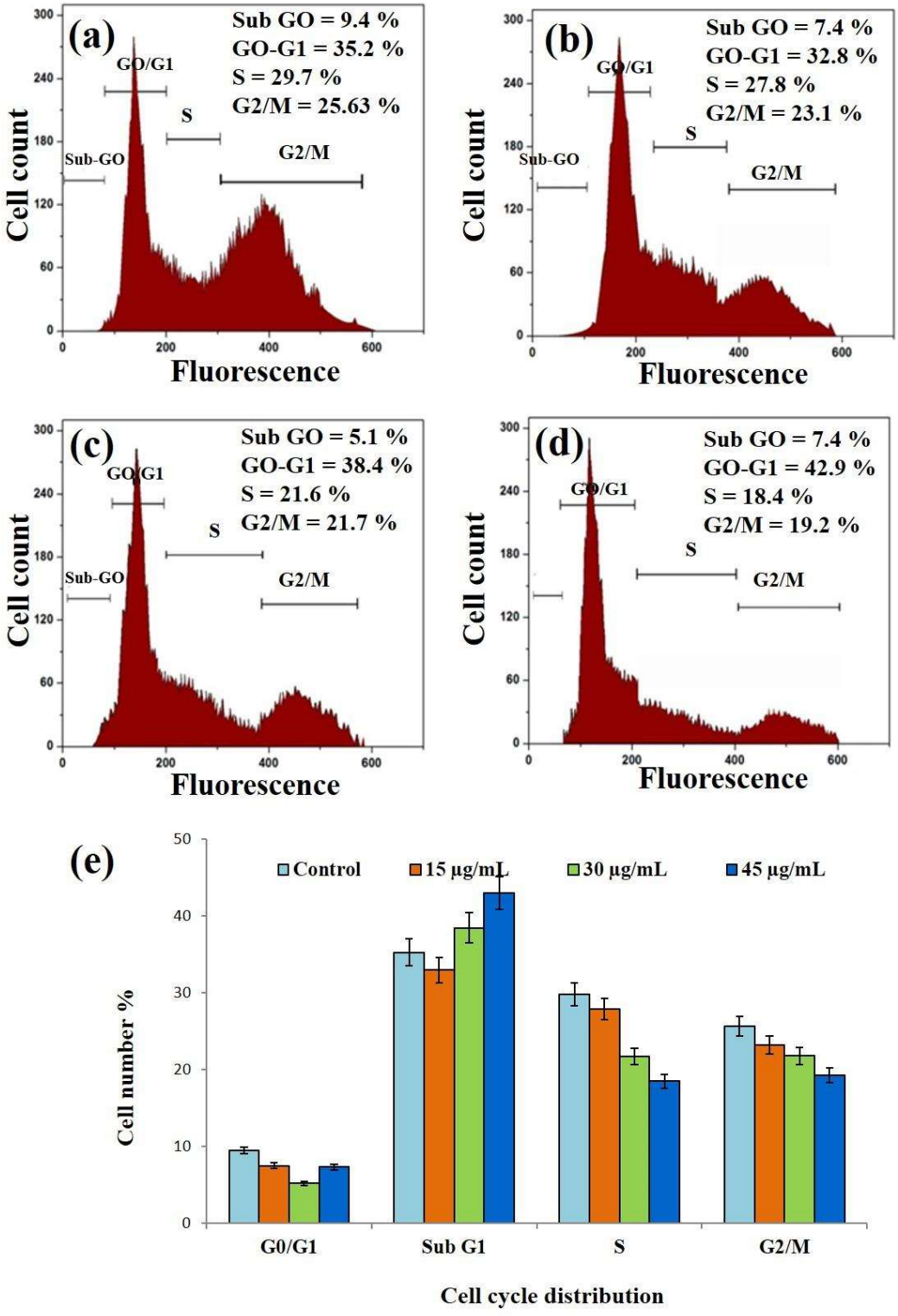

Figure 6.

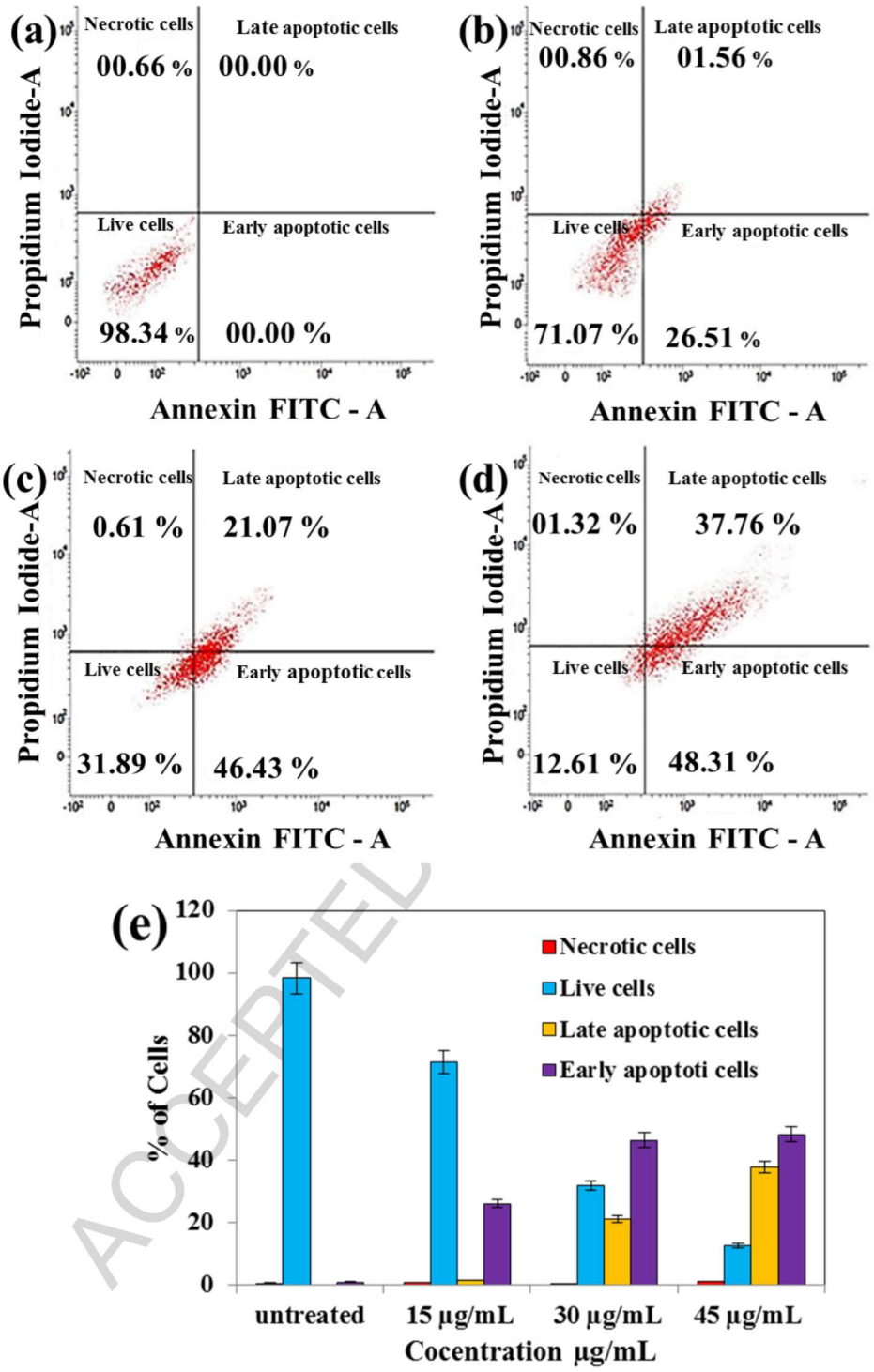

Figure 7.

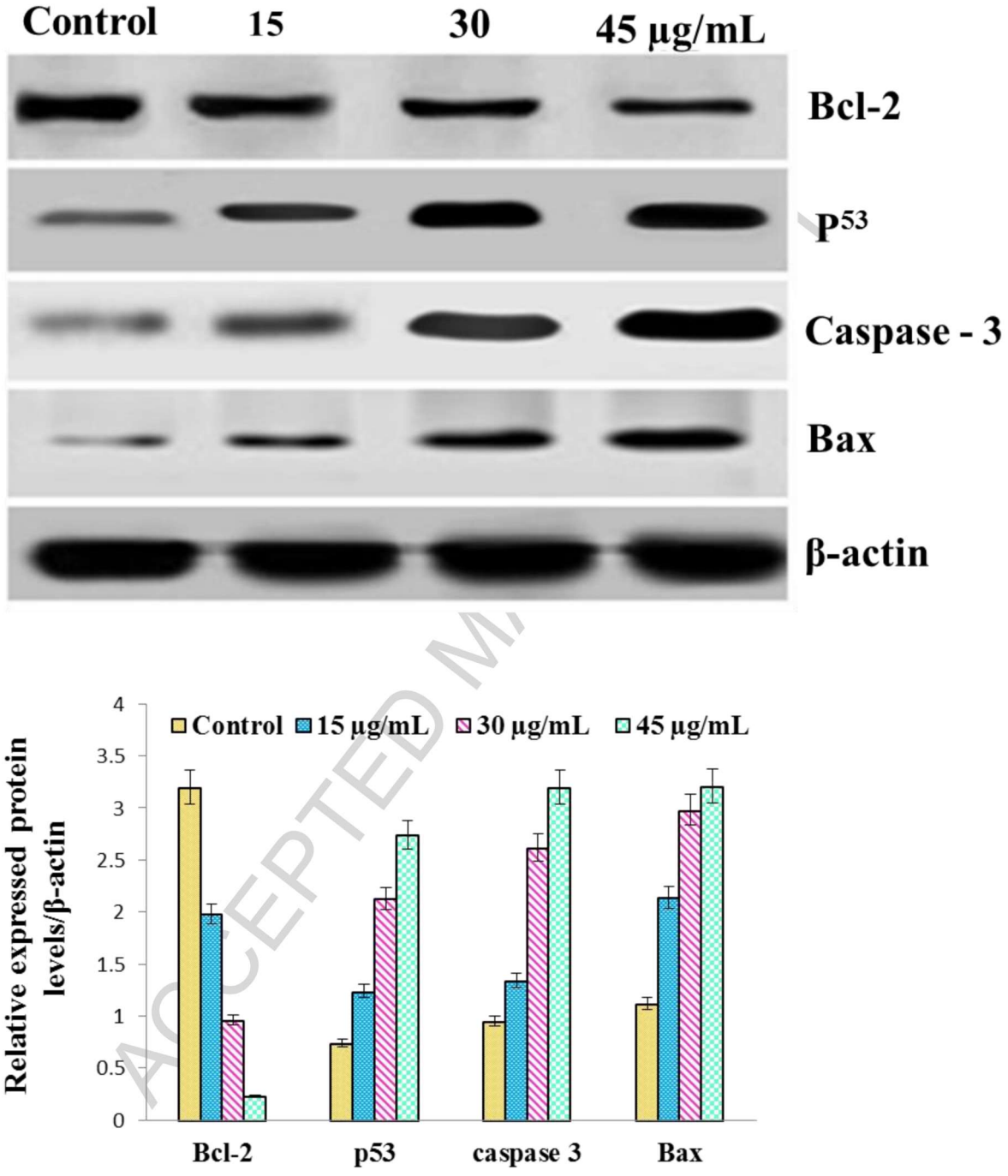

Figure 8.

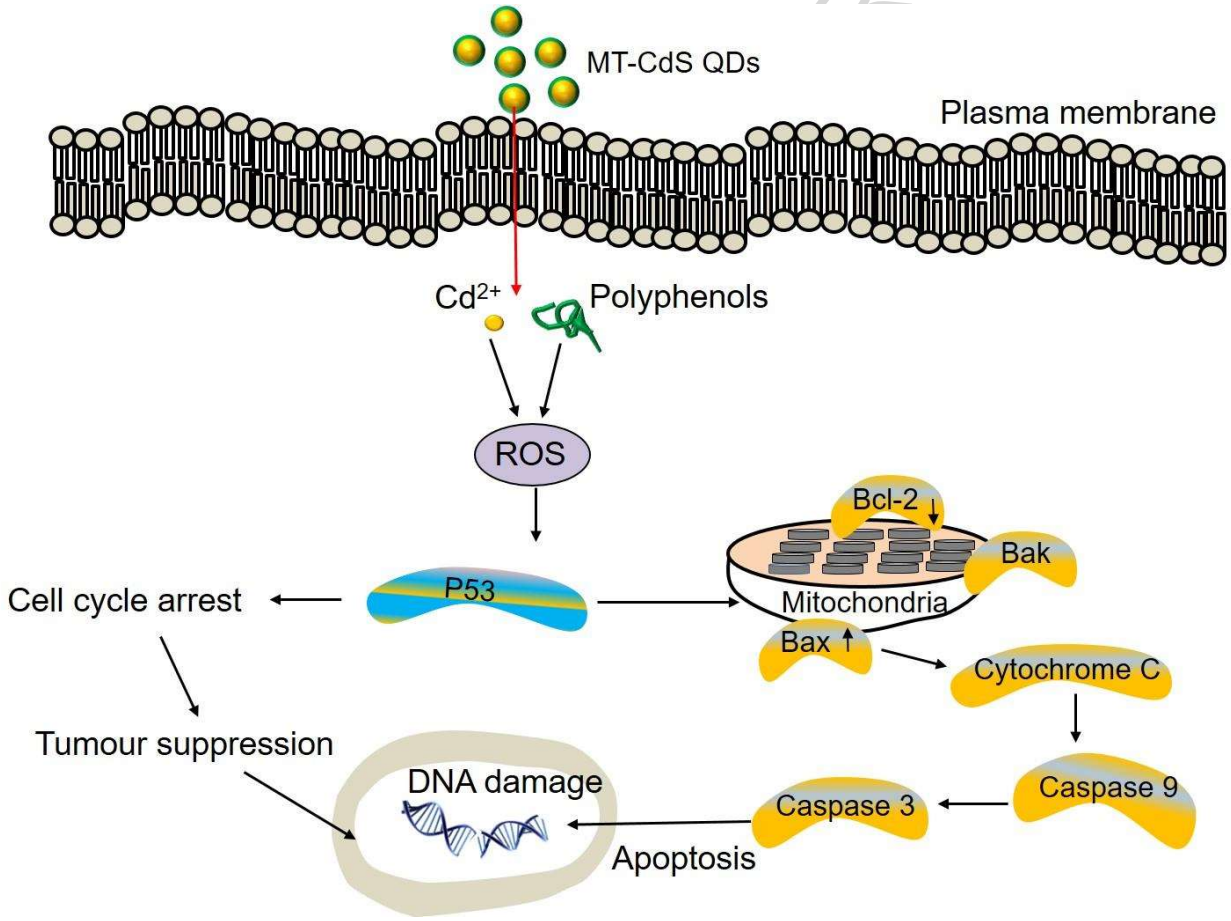

Scheme.1

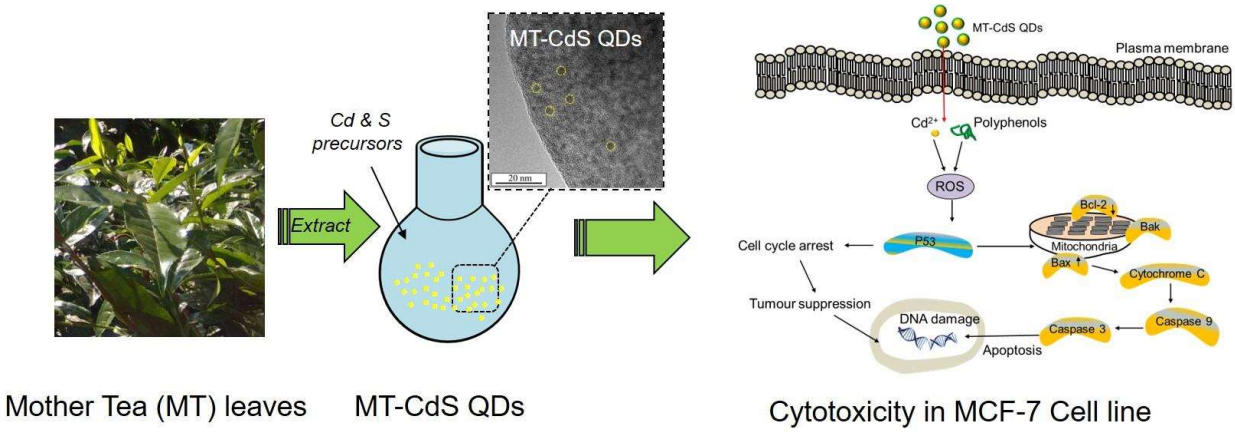

Graphical abstract

Highlights

- Recycling waste tea leaves based QDs synthesis has been demonstrated.
- Structure, optical, and chemical environment of tea leaves mediated QDs was studied.
- As synthesized QDs are lies between 2-4 nm size and showed effective fluorescence light emission.
- Tea leaves mediated QDs has potential to induce cell death in breast cancer cells at 24 hours.
- Ecofriendly, less expensive, green synthesized QDs can be apply in wide range of other applications.